Polymer Degradation and Stability 198 (2022) 109880

Contents lists available at ScienceDirect

Polymer Degradation and Stability

journal homepage: www.elsevier.com/locate/polymdegradstab

Advanced and traditional processing of thermoplastic polyurethane waste

Tamara Calvo-Correas[a,b,*], Miriam Benitez[a], Izaskun Larraza[a], Lorena Ugarte[a,c], Cristina Peña-Rodríguez[a], Arantxa Eceiza[a,*]

[a] 'Material + Technologies' Research Group (GMT), Department of Chemical and Environmental Engineering, Faculty of Engineering of Gipuzkoa, University of the Basque Country, Plaza Europa 1, Donostia-San Sebastian, 20018, Spain
[b] Department of Environmental Engineering, Faculty of Engineering of Vitoria-Gasteiz, University of the Basque Country, Nieves Cano street,12, Vitoria-Gasteiz, 01006, Spain
[c] Department of Graphical Expression and Project Management, Faculty of Engineering of Gipuzkoa, Eibar Section, University of the Basque Country, Otaola Hiribidea 29, Eibar, 20600, Spain

ARTICLE INFO

Article history:
Received 12 November 2021
Revised 24 February 2022
Accepted 1 March 2022
Available online 3 March 2022

Keywords:
Thermoplastic polyurethane
Mechanical recycling
Mechanical processing
3D printing
Electrospinning

ABSTRACT

In this work different ways to valorise discarded ear tags made of TPU from livestock sector were studied. This singular residue does not require separation from other plastics like other industrial and urbane wastes, which could contribute to simplify its management. Firstly, mechanical processing was carried out by several cycles of consecutive extrusion and injection processes. The material obtained in each process was characterized using different physical, chemical and mechanical characterization techniques in order to study the degradation as a consequence of processing cycles. Thereafter, suitable filaments for 3D printing were obtained and the effect of infill pattern in the mechanical properties of the printed pieces was investigated. Besides, an electrospun mat constituted by TPU waste microfibers was successfully obtained by electrospinning, and its morphology together with superficial and mechanical properties were characterized. Results showed that these applications were suitable options to valorise TPU waste consisting of discarded ear tags.

1. Introduction

In 2018, 359 million tonnes of plastic were produced worldwide, of which 61.8 million tonnes were generated in Europe. In Europe, only a 47% of post-consumed plastic waste were collected, being the 32.5% recycled, 42.6% used for energy recovery and 24.9% landfilled [1]. Among plastics, polyurethanes are the fifth most produced polymer in Europe and they are placed in seventh position worldwide [2]. Nowadays the consumption of PU in Europe is approximately of 3 million tonnes; being foams the 67% and elastomers the 6% [3,4]. Therefore, due to the current demand, as well as the directives of the European Union regarding the recycling of plastics for 2050 [5], the interest on recycling them in a suitable and efficient way has been skyrocketed amongst the scientific community. The methods of recycling polyurethane include energy recovery [6], physical or mechanical recycling [7] and chemical recycling [8]. Physical recycling consists in the direct reuse of plastic wastes without modifying their properties. Chemical recycling is following the degradation principle, the wastes are depolymerized for obtaining original reactants, other oligomers or small molecule organic compounds [9].

As aforementioned, the majority of the produced polyurethanes are thermostable, therefore chemical recycling is the most employed technique [10], especially glycolysis [11]. Nevertheless, although the amount of the produced thermoplastic polyurethanes (TPUs) is much lower, there is an interest also on finding a valid recycling route for TPUs wastes. For instance, in livestock sector, the ear tags used for identify bovine animals cannot be reused according to the second article of the Commission Regulation (CE) No 911/2004 of April 29, 2004, published in the Official Journal of the European Union [12]. Thus, they are discarded as non-toxic industrial waste without receiving any specific treatment and as far as authors know, nowadays no technique has been developed for its reuse. Therefore, in this work different suitable and efficient mechanical recycling routes of these residues were investigated.

* Corresponding author.
E-mail addresses: tamara.calvo@ehu.eus (T. Calvo-Correas), arantxa.eceiza@ehu.eus (A. Eceiza).

https://doi.org/10.1016/j.polymdegradstab.2022.109880

Due to its many advantages, such as being the most economical process and its high ecological and energetic efficiency, mechanical recycling is the most desirable technique [13]. Usually, plastics are grinded and processed through a physical process, i.e. compression [14], extrusion [5] and injection moulding [6]. However, the material cannot be subjected to extensive reprocessing cycles, since the processability and quality of end products can be compromised [15]. In each processing cycle the material can undergo irreversible thermal and mechanical degradation, which lead to physical and chemical changes and a detriment of final properties [16,17]. Thus, it is of utmost importance to know the number of reprocessing cycles to which the material can be exposed. Extrusion moulding can be used for the production of filaments for subsequent processing by 3D printing.

Furthermore, since additive manufacturing or 3D printing provides new opportunities for the manufacturing of components with customisable geometries and mechanical properties [18], the interest on this technique is increasing exponentially. Amongst the different 3D printing techniques, fused deposition modelling (FDM) is the most common [19]. FDM consists of the extrusion of a semi-molten filament through a heated nozzle to obtain a 3D object modelled by computer aided design (CAD). The material is deposited layer-by-layer onto a platform, where the material is cooled, solidified, and bonded with the surrounding layers [20]. Besides, mechanical properties of the manufactured object are not only controlled by the material of the filament, but also by the alignment of the deposited material during printing [21]. The mechanical properties of the printed object would be different depending on the direction, since the structure is composed by anisotropic layers [22]. Therefore, it is important to study the influence of different printing parameters such as layer thickness [23], processing temperature [24], infill percentage [22], type of material [25] and layer orientation [26,27] on the final mechanical properties of the objects.

Electrospinning could also be another interesting recycling route for thermoplastic waste. This technique leads the obtaining of mat of fibres, with diameters range from nanometres to micrometres, from a polymer solution induced by an electric field [28]. The polymer solution is stretched forming a nanofiber due to the potential difference between the collector and the spinneret. During this process, the solvent is evaporated, resulting in fibre mats [29]. This technique provides specific characteristics to the fabricated mats such us large surface area per unit area, porosity and a series of mechanical properties (flexibility and high tensile strength), being attractive at for advanced technological applications such as filtration, tissue engineering scaffolding and protective clothing [30–32]. Among the properties that determine the suitability of a material to be processed by the aforementioned advanced processing techniques, the molecular weight could be considered as a key parameter. Variation of this parameter will have a big influence on properties such as viscosity and melt strength [33,34].

The main goal of this study was to find suitable recycling routes for thermoplastic polyurethane wastes from livestock sector. To that end, the waste was subjected to several consecutive extrusion and injection processes and the degradation after each cycle was analysed. Besides, the obtained recycled TPU was processed by advanced processing techniques such as 3D printing and electrospinning. The extruded filaments were 3D printed and the effect of infill pattern in the final properties of the printed pieces was analysed. Furthermore, a TPU micro/nanofibers mat was developed by electrospinning technique. The effect of processing degradation as well as the properties of 3D printed material and obtained electrospun mat were characterized using Fourier transform infrared spectroscopy (FTIR), gel permeation chromatography (GPC), differential scanning calorimetry (DSC), thermogravimetric analysis (TGA), mechanical tests, optical microscopy (OM), scanning electron microscopy (SEM) and water contact angle (WCA).

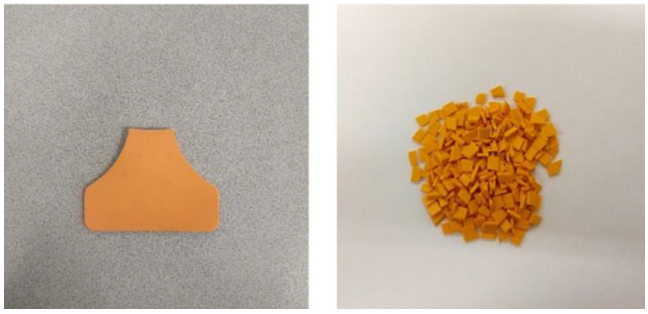

Fig. 1. Bovine ear tag: cleaned (left) and grinded (right).

2. Experimental

2.1. Materials

Discarded bovine ear tags made of thermoplastic polyurethane were collected from a slaughterhouse. Prior to mechanical recycling the ear tags were washed with pressurized water and hand soap to remove dirt, hair and other debris, to avoid they could interfere in the subsequent recycling process. The obtained clean ear tags were orange, flexible and light. The black ink used for the identification of cattle was not removed. The cleaned ear tags were grinded for its further utilization (Fig. 1).

To prepare solutions for electrospinning, tetrahydrofuran (THF) (HPLC grade) from Macron Fine Chemicals and N,N-dimethylformamide (DMF) (synthesis grade, >99.5%) supplied by Scharlau were employed as solvents.

2.2. Mechanical recycling process

The mechanical recycling process was carried out performing several consecutive extrusion and injection cycles, which are the most used technologies for plastic transformation.

Extrusion was carried out at 50 rpm in a HAAKE MiniLab twin screw extruder at a temperature of 210 °C, and a feeding rate of 0.3 g every 20 s using a nozzle with a diameter of 1.75 mm. The obtained filament had a diameter of 1.60 mm. Whereas, injection was held using a MiniJet HAAKE injector at a temperature of 210 °C, a pressure of 650 bar and a mould temperature of 50 °C, obtaining dog-bone shaped specimens.

The material was mechanically processed through a several stage process, summarized in Scheme 1. The process consisted on 3 extrusion and 4 injection stages, where the obtained filament after each extrusion stage was grinded and reused in the next extrusion stage as well as injected. Samples were coded as I (injection) and Ey (extrusion), being y the number of extrusion stages applied

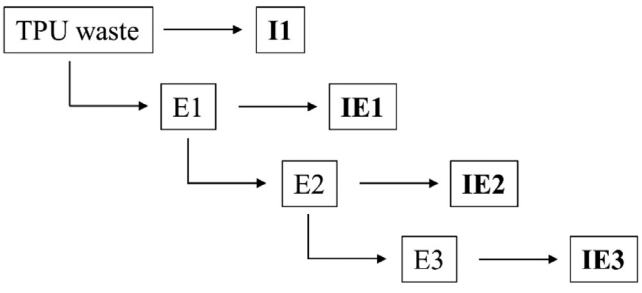

Scheme 1. Diagram of the performed mechanical recycling process.

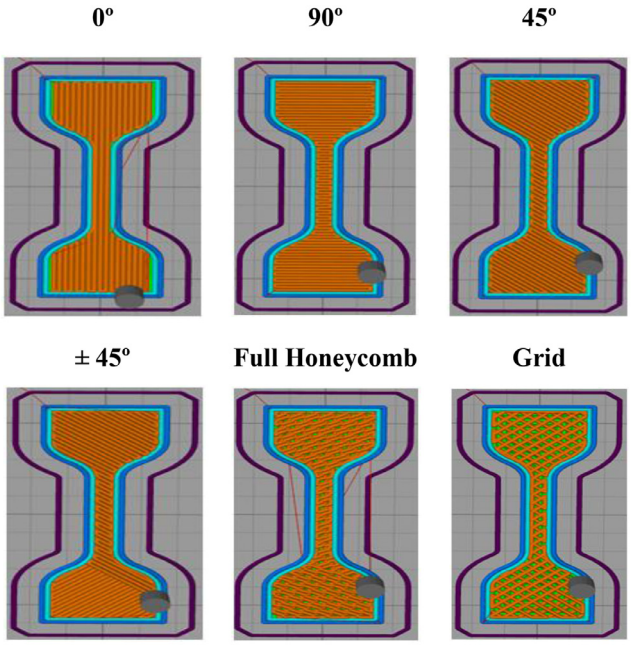

Fig. 2. 3D printing infill patterns.

to the sample, for example IE2 denotes that the injected material was previously subjected to 2 consecutive extrusion stages. In order to maximize the amount of waste that could be valorised, the 100% of the waste material was reused although TPU manufactures delimit the reuse of the material to 30%.

2.3. 3D printing

3D printing was carried out using the extruded filament E1 in a Tumaker Voladora NX printer by fused deposition modelling (FDM) technology. The parameters of the printing process and printed piece include thickness of the layers, number of shells, extrusion temperature, speed and nozzle diameter, amongst others. In this work, infill type was varied to study its influence on the mechanical properties of the printed piece. Printed samples had dog-bone shape, with dimensions of length, width and thickness of 50 mm, 10 mm and 2 mm, respectively.

In order to analyse the effect of the infill pattern on the mechanical properties, samples were printed using six different infill patterns (0°, 90°, 45°, ±45°, Full Honeycomb, Grid). In Fig. 2a scheme of each infill type for a single layer of deposited material is shown. Therefore, to be able to study the effect of the variation of the infill pattern, the printing parameters gathered in Table 1 were kept constant. In all cases, the outer layer was orientated at 45°.

2.4. Electrospinning

Randomly orientated fibres were electrospun by applying a voltage between 5 and 30 kV to the needle using a Fluidnatek LE-10 (Bioinicia) electrospinning equipment. The ground plate (stainless steel sheet on a screen) was placed at 15 cm from the needle tip (21-gauge blunt-end). The syringe pump delivered the polymer solution at a variable flow rate between 1 and 10 h^{-1}. The best solutions were collected for 2 h on the screen in order to produce an electrospun mat. The electrospinning process was controlled by observing the output of the dispersion from the needle tip by an optical microscope.

Five different solutions were prepared with different solvents (THF and DMF individually and mixtures of both) at the following concentrations: TPU at 10 wt% in THF (T-TPU10), TPU at 10 wt% in DMF (D-TPU10), TPU at 10 wt% in a THF/DMF mixture at a molar ratio 2:1 (2TD-TPU10) and TPU at 15 wt% in a THF/DMF mixture at a molar ratio 2:1 (2TD-TPU15). The solutions were subjected to a magnetic stirring for 24 h before loading in the electrospinning syringe.

Table 1
3D printing parameters.

Extruder temperature (°C)	220
Heated bed temperature (°C)	60
Print speed (mm s^{-1})	10
Nozzle diameter (mm)	0.60
Layer height (mm)	0.2
Infill percentage (%)	80

2.5. Characterization techniques

2.5.1. Fourier transform infrared spectroscopy (FTIR)

The identification of polyurethane characteristic functional groups was carried out by FTIR in attenuated total reflectance (ATR) mode using a Nicolet Nexus FTIR spectrometer equipped with a MKII Golden Gate accessory with diamond crystal at a nominal incident angle of 45° and ZnSe lens. The spectra were obtained after 32 scans in a wavenumber range from 4000 to 650 cm^{-1} with a resolution of 4 cm^{-1}.

2.5.2. Gel permeation chromatography (GPC)

The weight average molecular weight ($\overline{M_w}$), the number average molecular weight ($\overline{M_n}$) and the polydispersity index (PDI) of the raw TPU waste and the samples subjected to each extrusion and injection stage were determined by GPC using a Thermo Scientific chromatograph equipped with an isocratic Dionex UltiMate 3000 pump and a RefractoMax 521 refractive index detector. The separation was carried out at 30 °C within four Phenogel GPC columns from Phenomenex, with 5 µm particle size and 10^5, 10^3, 100 and 5 Å porosities, respectively, located in an UltiMate 3000 Thermostated Column Compartment. THF was used as mobile phase at a flow rate of 1 mL min^{-1}. Samples were prepared by dissolving them in THF at 1 wt% and filtering using 2 µm pore size nylon filters. Results were reported to as weight average polystyrene (PS) standards.

2.5.3. Differential scanning calorimetry (DSC)

Thermal properties were investigated by DSC using a Mettler Toledo DSC3+ equipment. Samples with a weight between 5 and 10 mg were sealed in aluminium pans. First, samples were heated from −80 °C to 240 °C at a scanning rate of 20 °C min^{-1} in N_2 (20 mL min^{-1}). After that, samples were cooled down and a second heating scan was performed from −80 °C to 240 °C at 10 °C min^{-1} in N_2 (20 mL min^{-1}). The inflection point of heat capacity change observed in the second scan was chosen to evaluate glass transition temperature (Tg) and melting temperature (Tm) was settled as the maximum of endothermic peak taking the area under the peak as melting enthalpy (ΔHm).

2.5.4. Thermogravimetric analysis (TGA)

The thermal stability of TPU samples was analysed in a Mettler Toledo TGA/SDTA851 thermogravimetric analyser. Samples of 5–10 mg were heated from 25 °C to 800 °C at a scanning rate of 10 °C min^{-1} under a nitrogen atmosphere (20 mL min^{-1}), as well as in air (20 mL min^{-1}) in order to simulate the mechanical recycling conditions. This technique determines the weight losses due to the volatile elimination and degradation, being able to relate them with the chemical structure. The starting point of thermal

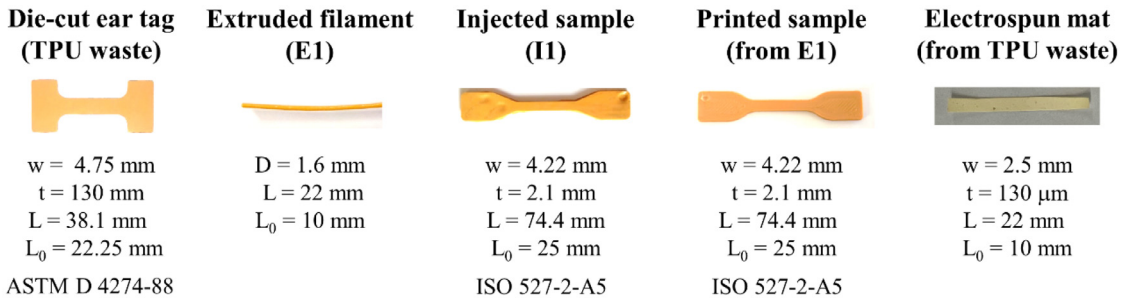

Fig. 3. Different samples used for the mechanical behaviour analysis and their dimensions.

degradation was defined as 5% weight loss and the degradation maximum temperature was determined as the minimum peak of the thermogravimetric derivative (DTG) curve.

2.5.5. Mechanical properties

Mechanical behaviour of TPU waste, extruded filaments, injected and 3D printed samples and electrospun mat was evaluated using an Instron 5967 testing machine provided with a 500 N load cell. Pneumatic grips of 1 kN were used to hold the test specimens. The dimensions of the samples are detailed in Fig. 3, being w (width), t (thickness), D (diameter) and L_0 (initial length) the parameters used for the determination of the mechanical properties. Tests were performed with a crosshead rate of 50 mm min^{-1} and in the case of the electrospun mat it was set at 5 mm min^{-1}. Elastic modulus (E), tensile strength (σ), and elongation at break (ε) were averaged from five specimen data.

2.5.6. Morphology of the electrospun mat

The morphology of the electrospun mat was analysed by optical microscopy (OM) and scanning electronic microscopy (SEM). For OM, the mat was analysed using an Eclipse E80i (Nikon) optical microscope, with 5x, 10x, 50x and 100x lenses. Regarding SEM, a Hitachi S-4800 Scanning Electron Microscope (SEM) with cold cathode field emission cannon at 5 kV was used. To that end, the sample was sputtered with 15 nm of gold using an Ion Sputter Emitech K550X.

2.5.7. Water contact angle (WCA)

The surface properties of electrospun mat were studied by the measurement of the contact angle between the sample and a water drop using a SEO Phoenix Series P-300 OCA 20 Dataphysics. The test was performed with a deionized water drop (3 µL) and the contact angle was averaged from at least 10 measurement data.

3. Results and discussion

3.1. Mechanical recycling

In order to determine the possible thermal degradation during the different stages of the processing of the material, the thermal stability of the TPU waste and the most processed sample, i.e. IE3, were analysed by TGA in N_2 and air atmosphere (Fig. 4). It was observed that both samples were stable up to 300 °C. Both temperatures were above the employed processing temperature, denoting that the employed processing methods would not result in any degradation that causes weight loss. Samples tested under nitrogen atmosphere showed two step thermal decomposition. The first one centred around 340 °C was related to the thermal decomposition of urethane linkages [35] and the second one centred around 420 °C, to the thermal decomposition of the soft segment [36]. Moreover, the content of soft and hard segments in the TPU waste was estimated taking into account the weight loss ascribed to each

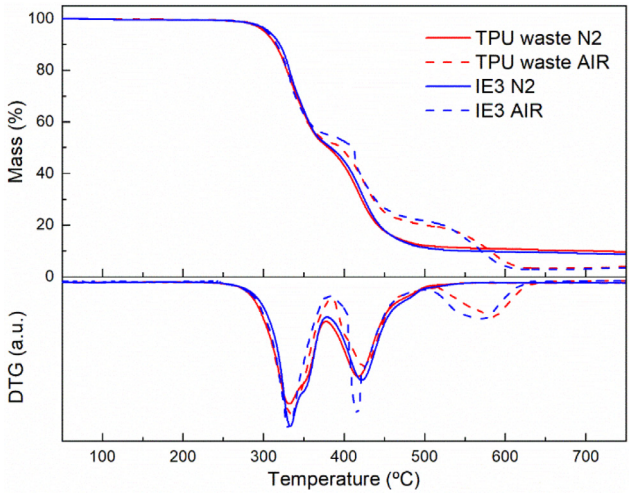

Fig. 4. Weight loss (up) and DTG (down) curves obtained for the TPU waste and IE3 sample.

segment, being around 55% for the HS and 45% for the SS. At air atmosphere three stages were observed, relating the first two to previously mentioned degradation of hard and soft segments, and the third stage with the loss of the formed carbonaceous material. Therefore, lower char content was observed in air atmosphere [36]. In this way, since both samples, TPU waste and IE3, showed similar thermogravimetric behaviour, it was concluded that the employed mechanical processing method did not provoke a degradation related with material weight loss .

The chemical structure evolution of the TPU waste during mechanical recycling was followed by FTIR, as can be observed in Fig. 5, where the spectra of TPU waste and the most processed IE3 sample are shown. TPU waste sample showed the characteristic bands of aromatic polyether polyurethanes [37]. The observed bands at 3300 and 1526 cm^{-1} were ascribed to stretching and bending vibrations of N–H bond of the urethane groups, respectively [11]. Moreover, the bands associated to stretching vibrations of C–N bond were observed at 1309 and 1220 cm^{-1} [38,39]. Furthermore, the characteristic band of the hydrogen-bonded carbonyl groups (C = O) in the crystalline region was seen at 1700 cm^{-1}, while the one ascribed to free carbonyl groups was observed at 1720 cm^{-1} [37]. The band centred at 1600 cm^{-1} was attributed to aromatic ring constituted in the hard segment [40], denoting that the used TPU waste was synthesised from an aromatic diisocyanate. Finally, the bands centred at 1100 and 1075 cm^{-1} corresponded to the stretching vibration of asymmetric C–O-C stretching of polyether and urethane, respectively [38].

Regarding the spectrum of IE3, no new bands were observed and all the characteristic bands were kept at the same wavenum-

Table 2
Thermal transition temperature and melting enthalpies of TPU waste and processed samples.

Sample	Tg_{SS}[°C]	Tg_{HS}[°C]	Tm_1[°C]	ΔHm_1[J/g]	Tm_2[°C]	ΔHm_2[J/g]
TPU waste	−49.4	54.1	122.1	2.3	208.4	12.1
I1	−49.2	60.6	121.7	2.7	203.7	14.0
E1	−48.7	59.6	122.7	1.9	201.7	13.0
IE1	−42.4	60.8	122.4	1.9	201.7	14.1
E2	−38.0	60.9	122.4	1.4	199.7	13.2
IE2	−44.4	60.3	121.1	1.6	199.1	12.3
E3	−30.9	59.1	121.8	1.4	196.9	15.6
IE3	−48.2	60.4	121.7	1.5	197.7	14.9

ber with similar intensity, suggesting that chemical structure was not altered.

Thermal properties of the samples were analysed by DSC after each mechanical processing stage. The thermal transition temperatures and melting enthalpies are gathered in Table 2. All samples presented two glass transition temperatures associated with soft and hard domains, Tg_{SS} and Tg_{HS}, respectively. Besides, two melting temperatures were observed, Tm_1, attributed to the melting of short-range ordered hard segment domains, and Tm_2, attributed to the melting of long-range ordered hard segment domains [41]. The existence of transitions ascribed to different domains suggested that the TPU used in ear tags presented a phase separated microstructure [10], as previously observed.

TPU waste showed Tg_{SS} and Tg_{HS} at −50 and 54 °C, respectively, and Tm_1 and Tm_2 at 122 and 208 °C, respectively. Therefore, samples were processed at 210 °C, which is above Tm_2. Regarding mechanically processed samples, in the case of I1 and E1 samples, which were the less processed ones, it was observed a decrease in the melting temperature of the long-range ordered domains (Tm_2) and an increase in the corresponding melting enthalpy (ΔHm_2). This fact suggested a higher crystallinity in the hard domain, but at the same time, smaller size of crystalline structures, which could trigger the observed Tg_{HS} increase. This fact could be attributed to the chain excision occurring during the processing, since the structural degradation of polyurethanes may include chain scission [42], giving place to shorter chains with higher mobility capable to crystallize. In the case of the most processed samples (from IE1 to IE3), in addition to the changes observed for I1 and E1 samples, an increase in the Tg_{SS} and a decrease in the short range ordering domains enthalpy (ΔHm_1) was also observed, suggesting the occurrence of a microphase mixing caused by a more severe chain scission.

The mechanical properties of the TPU waste, as well as the processed materials were analysed by tensile test Table 3. summarizes

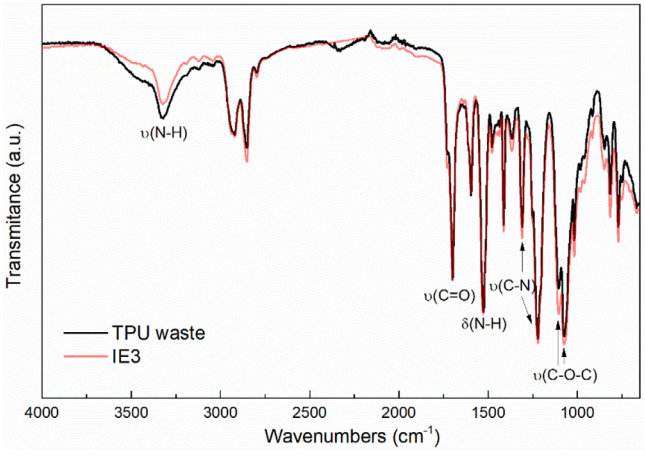

Fig. 5. FTIR spectrum obtained for TPU waste and most processed IE3 sample.

Table 3
Mechanical properties: Young modulus (E), tensile strength (σ) and elongation at break (ε).

Sample	E [MPa]	σ [MPa]	ε[%]
TPU waste	58.4 ± 4.2	41.3 ± 4.4	802.4 ± 43.8
I1	43.3 ± 2.4	37.8 ± 1.5	970.3 ± 18.0
E1	66.9 ± 2.7	39.0 ± 1.3	964.5 ± 28.8
IE1	68.3 ± 4.2	19.7 ± 1.0	571.9 ± 19.3
E2	94.8 ± 4.3	19.9 ± 0.5	424.4 ± 11.3
IE2	70.1 ± 4.3	13.0 ± 0.7	415.9 ± 33.8
E3	95.3 ± 7.9	11.2 ± 0.3	205.3 ± 37.8
IE3	66.0 ± 7.8	8.6 ± 0.2	186.3 ± 24.6

the measured Young modulus (E), tensile strength (σ) and elongation at break (ε) values. Regarding mechanical properties, differences were appreciated between less processed (I1 and E1) and more processed samples (IE1-IE3). It was seen that the mechanical properties of I1 and E1 were in the range of the ones of TPU waste, as also shown in stress-strain curves represented in Fig. 6, meaning that the subjected mechanical processing did not modify significantly the performance of the I1 and E1 materials. However, as can be observed in the mechanical properties gathered in Table 3, the increase of processing stages resulted in a detriment of tensile strength and elongation at break values, probably due to the chain excision effect denoted in DSC analysis. The increase of crystallinity of hard domains together with the decrease crystal size would explain the increase in Young modulus resulting in a more rigid but fragile material. This fact denoted a degradation of the material as a consequence of processing.

In order to confirm the degradation due to the chain excision and a possible weight loss caused by mechanical processing, all the obtained samples were analysed by GPC and results are shown in Table 4. Although I1 and E1 showed lower $\overline{M_n}$ and $\overline{M_w}$ values than TPU waste, still were quite high to maintain similar thermal and mechanical properties to those observed for the TPU waste. However, with the increase of the mechanical processing stages, the, $\overline{M_n}$ and $\overline{M_w}$ decreased gradually, affecting negatively to the final properties as observed in thermal and mechanical behaviour, and confirming the degradation of the material. Furthermore, the polydispersity index showed a tendency to increase with the in-

Table 4
Weight average molecular weight ($\overline{M_w}$), number average molecular weight ($\overline{M_n}$) and polydispersity index (PDI) of all the samples determined by GPC.

Sample	$\overline{M_n}$ [g mol^{-1}]	$\overline{M_w}$ [g mol^{-1}]	PDI
TPU waste	69,293	99,405	1.4362
I1	48,924	71,858	1.4688
E1	48,316	67,025	1.3872
IE1	42,348	59,016	1.3936
E2	39,943	54,361	1.3610
IE2	27,476	42,376	1.5423
E3	27,187	41,182	1.5148
IE3	20,061	35,467	1.7680

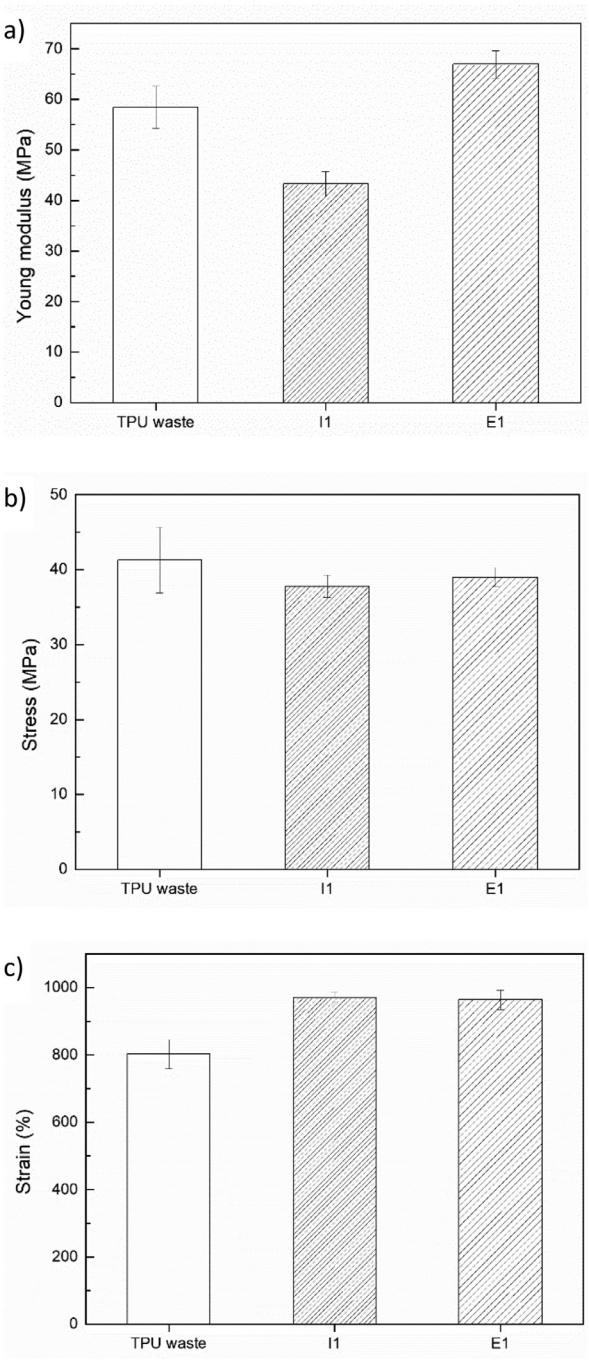

Fig. 6. Mechanical properties of TPU waste, E1 and I1: a) Young modulus, b) stress and c) strain.

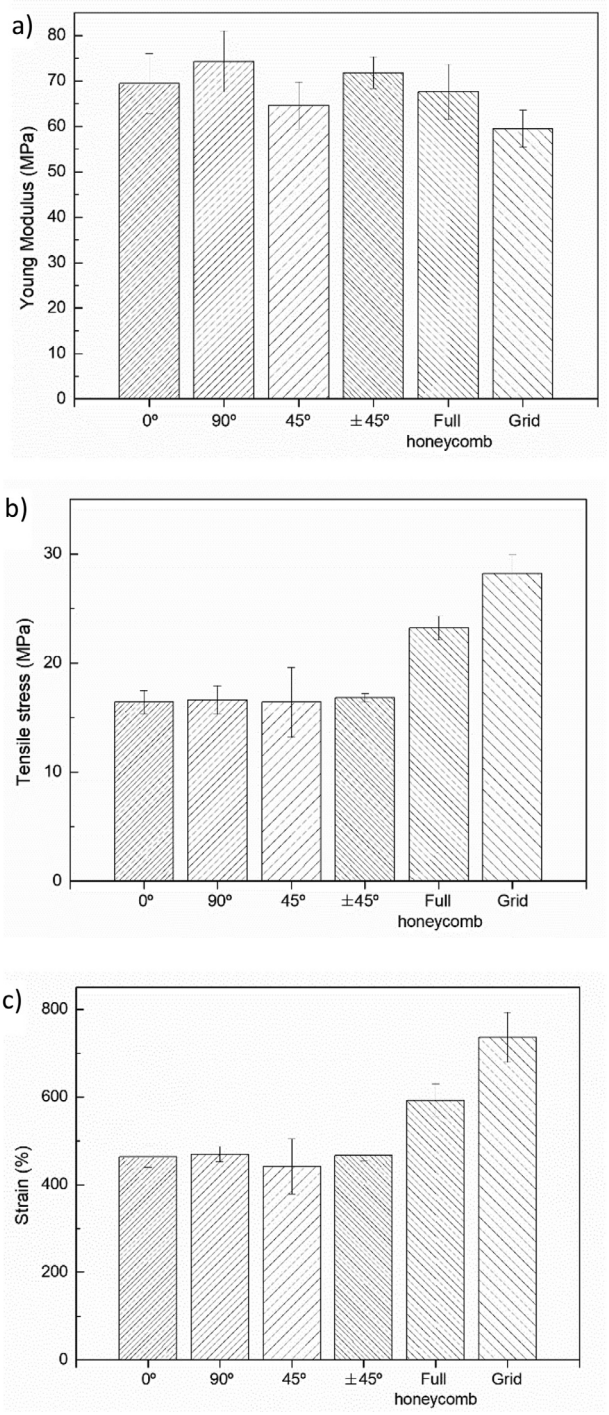

Fig. 7. Mechanical properties of 0°, 45°, 90°, ± 45°, full honeycomb and grid: a) Young modulus, b) stress and c) strain.

crease in processing steps. This was related to the increase on chain length heterogeneity due to the random chain excision and degradation.

3.2. 3D printing

In sight of the obtained results, it was concluded that the most suitable material to be reprocessed by 3D printing was the filament obtained after a single extrusion, E1, due to its lower degradation and final properties. As previously observed, E1 showed the highest molecular weight amongst the processed filaments, which suggested a higher entanglement of the chains and thus resulting in a higher melting strength. Therefore, E1 was the most suitable material for 3D printing. The lower molecular weight observed for E2 and E3 filaments denoted higher level of degradation by chain scission and consequently their melt strength would not be adequate to be printed.

As can be observed in Fig. 3, E1 is suitable for 3D printing. Samples with different infill patterns were printed successfully. All samples were printed using the same printing parameters, so all of them experienced the same thermal history. Tensile tests of the printed samples were performed in order to analyse the influence of the infill. The obtained results are gathered in Table 5 and stress-strain curves of 0°, 45°, 90°, ± 45°, full honey comb

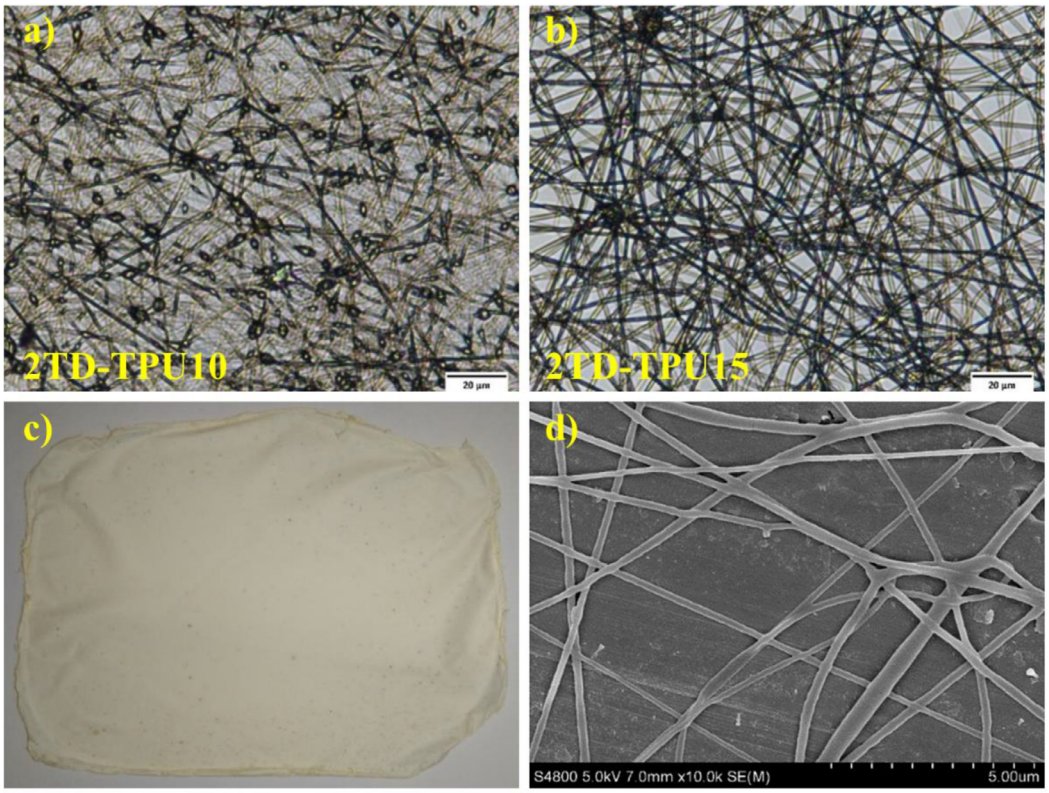

Fig. 8. Optical microscopy images at a magnification of 50x of: a) 2TD-TPU10 and b) 2TD-TPU15. c) Digital image of the electrospun mat from 2TD-TPU15 (sample size 10 cm x 7.5 cm) and d) SEM image of the obtained 2TD-TPU15 mat.

Table 5
Mechanical properties of 3D printed samples.

Sample	E [MPa]	σ [MPa]	ε [%]
TPU waste	58.4 ± 4.2	41.3 ± 4.4	802.4 ± 43.8
0°	69.4 ± 6.7	16.4 ± 1.1	463.5 ± 23.7
90°	74.3 ± 6.7	16.6 ± 1.3	469.6 ± 18.0
45°	64.6 ± 5.2	16.4 ± 3.2	441.9 ± 62.8
± 45°	71.8 ± 3.5	16.8 ± 0.4	466.4 ± 12.2
Full Honeycomb	67.6 ± 6.1	23.2 ± 1.1	592.1 ± 37.7
Grid	59.5 ± 4.1	28.2 ± 1.7	736.4 ± 56.7

and grid samples are shown in Fig. 7. As can be observed, samples printed at 0°, 45°, 90° and ± 45° showed similar properties in spite of the employed printing pattern. These results differed from the obtained by Lin et al. [43], where pieces printed at raster angle of 0° provided the best mechanical performance and highest degree of anisotropy. However, as Elmrabet et al. [44]. suggested, the infill settings variation has less effect in small sample geometries, which could had happened in the tested samples, since their cross section was small. Regarding the mechanical properties of printed samples with more complex patterns, i.e. full honeycomb and grid, higher values of strength and elongations at break were measured. Similar results were reported by Srinivasan et al. [45]. for printed pieces of polyethylene terephthalate glycol. This behaviour could be due to the stronger bonds produced in grid and honeycomb patterns. In addition, strength and elongation at break of the printed pieces using grid and full honeycomb pattern were higher to the IE1 or E2 samples (Table 3), which are reprocessed using the pelletized E1 filament.

3.3. Electrospinning

In order to find the most suitable solution for obtaining an electrospun mat from TPU waste, solvent, TPU waste content, voltage and flow were optimized. First of all, the most suitable solvent was chosen [46]. The polymer was solved in both THF and DMF, showing a good polymer solvent interaction since stable solutions were obtained. However, different drawbacks related to the boiling temperature of the solvents were observed. The fibres obtained from solutions using THF as solvent showed multiple imperfections, due to the solidification of the solution in the tip of the needle, according to the low boiling point and high volatility of the solvent. Whereas, solutions prepared using DMF, which has a higher boiling point, were not able to be spun, due to the difficulty evaporating the solvent. Therefore, a solution of the polymer in a mixture of THF/DMF at a molar ratio of 2:1 was prepared obtaining results that are more favourable. Regarding TPU waste content, as it was observed in Fig. 8a and b, where optical microscopy images of solutions with 10 and 15 wt% of TPU waste are shown, it was seen that the increase of the content of the TPU lead to the obtaining of fibres with less imperfections. This effect could be indicative of a higher solution viscosity, which impeded the scattering the extruded jet and, thus, allowed the obtaining of more homogenous and continuous fibres. In addition, the use of a solution with a higher amount of polymer allowed a higher valorisation of the TPU waste. As shown in Fig. 8c, a electrospun mat of 130 μm of thickness was obtained from a solution of 15 wt% TPU in a mixture of THF/DMF in a 2:1 ratio, 2TD-TPU15, after 2 h of collection. The morphology of the obtained mat was analysed by SEM (Fig. 8d). As can be observed, the TPU waste showed a suitable spinnability resulting in continuous fibres with smooth surface. The diameter of the fibres was less than 4 μm, denoting that the obtained mat was constituted by micro-fibres. Furthermore, the electrospun mat was mechanically characterized and the following values were determined: Young's modulus of 6.00 ± 0.88 MPa, stress at break of 4.72 ± 0.53 MPa and deformation at break of 102.22 ± 9.97%. As can be seen, the overall mechanical properties of the mat were lower than the ones of the neat TPU waste. This result was ex-

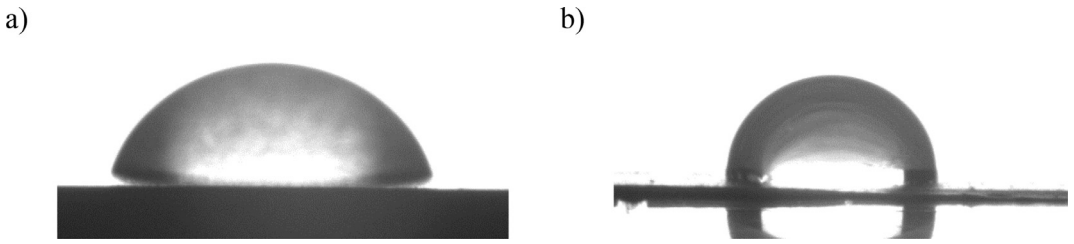

Fig. 9. Digital image of a water drop on top of a) neat TPU waste and b) 2TD-TPU15 electrospun mat.

pected due to the morphology of the mat, which was formed by non-woven micro-fibres instead of a continuous material. Finally, since this kind of electrospun material can found application as coating or textile amongst others, the water contact angle was measured, Fig. 9. The electrospun mat showed a water contact angle of 91.6 ± 2.7°, which was notably higher than the measured for the neat TPU waste (69.2 ± 1.3°). The increase of the hydrophobicity of the material could be ascribed to the inherent roughness of the nanofibers, which allowed the surface to entrap air [47].

4. Conclusions

In this work different mechanical processing stages (extrusion, injection and a combination of both) were used in order to valorise residues form livestock sector, i.e. ear tags for cattle identification made of TPU. The obtained materials after each processing stage were characterized. It was observed that the employed mechanical processing did not modify the chemical composition and neither the thermal stability. However, according to DSC analysis, the material withstood certain degradation, especially after several consecutive processing stages. This fact was also corroborated by the analysis of the mechanical properties and molecular weight, since a worsening of tensile properties and a decrease of the molecular weight were observed as the number of processing stages increased. The increase of crystallinity, stiffness and polydispersity, together with the decrease of tensile strength, ductility and molecular weight suggested that the material experienced chain scission during the mechanical processing, which was more severe as the number of mechanical processing stages increased. Nevertheless, when the residue was only processed in a single stage, extrusion or injection, the material was not degraded in a high extent and its properties were suitable for further application in advanced processing techniques. Besides, it should be highlighted that in this work the maximization of the amount of reused material was prioritised. For future research, it would be of interest to analyse the optimum recycling percentage prioritising the material performance. The recycled filament was proven suitable for 3D printing, where the best mechanical behaviour was observed for full honeycomb and grid infill patterns. Moreover, TPU waste was successfully employed in electrospinning technique, obtaining an electrospun mat of 130 μm constituted by microfibres of less than 4 μm of diameter. These two applications emerge as feasible routes to give value to the recollected agricultural residue, contributing to circular economy.

Declaration of Competing Interest

The authors declare that they have no known competing financial interests or personal relationships that could have appeared to influence the work reported in this paper.

CRediT authorship contribution statement

Tamara Calvo-Correas: Writing – original draft, Writing – review & editing, Supervision. **Miriam Benitez:** Writing – original draft, Investigation. **Izaskun Larraza:** Investigation. **Lorena Ugarte:** Writing – review & editing. **Cristina Peña-Rodríguez:** Supervision. **Arantxa Eceiza:** Writing – review & editing, Supervision.

Acknowledgements

Authors thank the University of the Basque Country (UPV/EHU) (GIU18/216 Research Group) and Eurorregion New Aquitaine - Basque Country - Navarre project (RECYCLEPOLYWASTE) for the financial support, as well as the technical support from “Macrobehavior-Mesostructure-Nanotechnology” and “Biomedicine microscopy” the SGIker units. Finally, T.C–C. thanks the UPV/EHU (ESPDOC19/41) and M.B. the Provincial Country of Gipuzkoa (2019-BE01–000004).

References

[1] Plastic Europe. Plastics - the facts 2019. https://www.plasticseurope.org/en/resources/publications/1804-plastics-facts-2019.
[2] Polyurethane production, pricing and market demand. https://www.plasticsinsight.com/resin-intelligence/resin-prices/polyurethane/.
[3] H.M.C.C. Somarathna, S.N. Raman, D. Mohotti, A.A. Mutalib, K.H. Badri, The use of polyurethane for structural and infrastructural engineering applications: a state-of-the-art review, Constr. Build. Mater. 190 (2018) 995–1014.
[4] Global polyurethane demand 2012-2022. https://www.statista.com/statistics/747004/polyurethane-demand-worldwide/.
[5] E. CommissionCommunication from the Commission to the European Parliament, the council, the European Economic and Social Committee and the Committee of the Regions, A european strategy for plastics in a circular economy, 2018.
[6] K.M. Zia, H.N. Bhatti, I.Ahmad Bhatti, Methods for polyurethane and polyurethane composites, recycling and recovery: a review, React. Funct. Polym. 67 (2007) 675–692.
[7] K. Ragaert, L. Delva, K. Van Geem, Mechanical and chemical recycling of solid plastic waste, Waste Manag 69 (2017) 24–58.
[8] X. Wang, H. Chen, C. Chen, H. Li, Chemical degradation of thermoplastic polyurethane for recycling polyether polyol, Fibers Polym 12 (2011) 857–863.
[9] W. Yang, Q. Dong, S. Liu, H. Xie, L. Liu, J. Li, Recycling and disposal methods for polyurethane foam wastes, Procedia Environ. Sci. 16 (2012) 167–175.
[10] D. Simón, A.M. Borreguero, A. de Lucas, J.F. Rodríguez, Recycling of polyurethanes from laboratory to industry, a journey towards the sustainability, Waste Manag 76 (2018) 147–171.
[11] T. Calvo-Correas, L. Ugarte, P.J. Trzebiatowska, R. Sanzberro, J. Datta, M.Á. Corcuera, A. Eceiza, Thermoplastic polyurethanes with glycolysate intermediates from polyurethane waste recycling, Polym. Degrad. Stab. 144 (2017) 411–419.
[12] Official Journal of the European Union, Commission regulation (EC) No 911/2004 of 29 April 2004, 2004.
[13] J. Maris, S. Bourdon, J.M. Brossard, L. Cauret, L. Fontaine, V. Montembault, Mechanical recycling: compatibilization of mixed thermoplastic wastes, Polym. Degrad. Stab. 147 (2018) 245–266.
[14] E. Leger, B. Landry, G. LaPlante, High flow compression molding for recycling discontinuous long fiber thermoplastic composites, J. Compos. Mater. 23 (2020) 3343–3350.
[15] P. Oblak, J. Gonzalez-Gutierrez, B. Zupančič, A. Aulova, I. Emri, Processability and mechanical properties of extensively recycled high density polyethylene, Polym. Degrad. Stab. 114 (2015) 133–145.
[16] A.F. Rojas González, L.M.A. Ríos, Estabilidad de procesamiento de polímeros: índice de degradación en proceso, Mutis 5 (2015) 37–45.
[17] I. Goitisolo, J.I. Eguiazábal, J. Nazábal, Effects of reprocessing on the structure and properties of polyamide 6 nanocomposites, Polym. Degrad. Stab. 93 (2008) 1747–1752.
[18] S. Garzon-Hernandez, D. Garcia-Gonzalez, A. Jérusalem, A. Arias, Design of FDM 3D printed polymers: an experimental-modelling methodology for the prediction of mechanical properties, Mater. Des. 188 (2020) 108414.
[19] T.D. Ngo, A. Kashani, G. Imbalzano, K.T.Q. Nguyen, D. Hui, Additive manufacturing (3D printing): a review of materials, methods, applications and challenges, Compos. Part B Eng. 143 (2018) 172–196.

[20] C. Bellehumeur, L. Li, Q. Sun, P. Gu, Modeling of bond formation between polymer filaments in the fused deposition modeling process, J. Manuf. Process. 6 (2004) 170–178.
[21] C. Ziemian, M. Sharma, S. Ziemi, Anisotropic Mechanical Properties of ABS Parts Fabricated by Fused Deposition Modelling, Mech. Eng., InTech, 2012 in: D.M.G. (Ed.) (Ed.).
[22] K.L. Alvarez C, R.F. Lagos C, M. Aizpun, Investigating the influence of infill percentage on the mechanical properties of fused deposition modelled ABS parts, Ing. e Investig. 36 (2016) 110–116.
[23] A. Kantaros, D. Karalekas, Fiber Bragg grating based investigation of residual strains in ABS parts fabricated by fused deposition modeling process, Mater. Des. 50 (2013) 44–50.
[24] I. Gajdoš, J. Slota, Influence of printing conditions on structure in FDM prototypes, Teh. Vjesn. 20 (2013) 231–236.
[25] G. Ćwikła, C. Grabowik, K. Kalinowski, I. Paprocka, P. Ociepka, The influence of printing parameters on selected mechanical properties of FDM/FFF 3D-printed parts, IOP Conf. Ser. Mater. Sci. Eng. 227 (2017) 0–10.
[26] V. Vega, J. Clements, T. Lam, A. Abad, B. Fritz, N. Ula, O.S. Es-Said, The effect of layer orientation on the mechanical properties and microstructure of a polymer, J. Mater. Eng. Perform. 20 (2011) 978–988.
[27] M. Lorenzo-Bañuelos, A. Díaz, I.I. Cuesta, Influence of raster orientation on the determination of fracture properties of polypropylene thin components produced by additive manufacturing, Theor. Appl. Fract. Mech. 107 (2020) 102536.
[28] A. Santamaria-Echart, L. Ugarte, K. Gonzalez, L. Martin, L. Irusta, A. Gonzalez, M.A. Corcuera, A. Eceiza, The role of cellulose nanocrystals incorporation route in waterborne polyurethane for preparation of electrospun nanocomposites mats, Carbohydr. Polym. 166 (2017) 146–155.
[29] C. Akduman, E.P.A. Kumbasar, Electrospun polyurethane nanofibers, Intech. (2017). https://doi.org/http://dx.doi.org/10.5772/intechopen.69937 23.
[30] A. Haider, S. Haider, I.K. Kang, A comprehensive review summarizing the effect of electrospinning parameters and potential applications of nanofibers in biomedical and biotechnology, Arab. J. Chem. 11 (2018) 1165–1188.
[31] F.A. Sheikh, N.A.M. Barakat, M.A. Kanjwal, A.A. Chaudhari, I.H. Jung, J.H. Lee, H.Y. Kim, Electrospun antimicrobial polyurethane nanofibers containing silver nanoparticles for biotechnological applications, Macromol. Res. 17 (2009) 688–696.
[32] L. Wang, S. Yang, J. Wang, C. Wang, L. Chen, Fabrication of superhydrophobic TPU film for oil-water separation based on electrospinning route, Mater. Lett. 65 (2011) 869–872.
[33] S. Mohammadzadehmoghadam, Y. Dong, I.Jeffery Davies, Recent progress in electrospun nanofibers: reinforcement effect and mechanical performance, J. Polym. Sci. Part B Polym. Phys. 53 (2015) 1171–1212.
[34] D.H. Reneker, A.L. Yarin, Electrospinning jets and polymer nanofibers, Polymer (Guildf) 49 (2008) 2387–2425.
[35] D. Allan, J. Daly, J.J. Liggat, Thermal volatilisation analysis of TDI-based flexible polyurethane foam, Polym. Degrad. Stab. 98 (2013) 535–541.
[36] D.K. Chattopadhyay, D.C. Webster, Thermal stability and flame retardancy of polyurethanes, Prog. Polym. Sci. 34 (2009) 1068–1133.
[37] L. Ugarte, B. Fernández-D'Arlas, A. Valea, M.L. González, M.A. Corcuera, A. Eceiza, Morphology-properties relationship in high-renewable content polyurethanes, Polym. Eng. Sci. 54 (2014) 2282–2291.
[38] A. Dannoux, S. Esnouf, J. Begue, B. Amekraz, C. Moulin, Degradation kinetics of poly(ether-urethane) Estane® induced by electron irradiation, Nucl. Instruments Methods Phys. Res. Sect. B Beam Interact. with Mater. Atoms. 236 (2005) 488–494, doi:10.1016/j.nimb.2005.04.025.
[39] M.R. Patel, J.M. Shukla, N.K. Patel, K.H. Patel, Biomaterial based novel polyurethane adhesives for wood to wood and metal to metal bonding, Mater. Res. 12 (2009) 385–393.
[40] P. Jutrzenka Trzebiatowska, A. Santamaria Echart, T. Calvo Correas, A. Eceiza, J. Datta, The changes of crosslink density of polyurethanes synthesised with using recycled component. Chemical structure and mechanical properties investigations, Prog. Org. Coatings. 115 (2018) 41–48.
[41] S. Yamasaki, D. Nishiguchi, K. Kojio, M. Furukawa, Effects of aggregation structure on rheological properties of thermoplastic polyurethanes, Polymer (Guildf) 48 (2007) 4793–4803.
[42] J.S. Stevenson, R.P. Kusy, Structural degradation of polyurethane-based elastomeric modules, J. Mater. Sci. Mater. Med. 6 (1995) 377–384.
[43] X. Lin, P. Coates, M. Hebda, R. Wang, Y. Lu, L. Zhang, Experimental analysis of the tensile property of FFF-printed elastomers, Polym. Test. 90 (2020) 106687.
[44] N. Elmrabet, P. Siegkas, Dimensional considerations on the mechanical properties of 3D printed polymer parts, Polym. Test. 90 (2020) 106656.
[45] R. Srinivasan, K. Nirmal Kumar, A. Jenish Ibrahim, K.V. Anandu, R. Gurudhevan, Impact of fused deposition process parameter (infill pattern) on the strength of PETG part, Mater. Today Proc. 27 (2020) 1801–1805.
[46] S. Torres-Giner, R. Pérez-Masiá, J.M. Lagaron, A review on electrospun polymer nanostructures as advanced bioactive platforms, Polym. Eng. Sci. 56 (2016) 500–527.
[47] E. Schoolaert, L. Cossu, J. Becelaere, J.F.R. Van Guyse, A. Tigrine, M. Vergaelen, R. Hoogenboom, K. De Clerck, Nanofibers with a tunable wettability by electrospinning and physical crosslinking of poly(2-n-propyl-2-oxazoline), Mater. Des. 192 (2020) 108747.